J. Fluid Mech. (1996), *vol.* 314, *pp.* 1–25

On the motion of three point vortices in a periodic strip

By HASSAN AREF AND MARK A. STREMLER
Department of Theoretical and Applied Mechanics, University of Illinois at Urbana-Champaign, Urbana, IL 61801-2935, USA

(Received 6 June 1995 and in revised form 16 November 1995)

Motivated by observations of Williamson & Roshko of the wake of an oscillating cylinder with three vortices per cycle, and by the analyses of Rott and Aref of the motion of three vortices with vanishing net circulation on the unbounded plane, the integrable problem of three interacting, periodic vortex rows is solved. The problem is 'mapped' onto a problem of advection of a passive particle by a certain set of fixed point vortices. The results of this mapped problem are then re-interpreted in terms of the motion of the vortices in the original problem. A rather complicated structure of the solution space emerges with a surprisingly large number of regimes of motion, some of them somewhat counter-intuitive. Representative cases are analysed in detail, and a general procedure is indicated for all cases. We also trace the bifurcations of the solutions with changing linear momentum of the system. For rational ratios of the vortex circulations all motions are periodic. For irrational ratios this is no longer true. The point vortex results are compared to the aforementioned wake experiments and appear to shed light on the experimental observations. Many additional possibilities for the wake dynamics are suggested by the analysis.

1. Introduction

Several investigators have explored the wake patterns formed by an oscillating cylinder in a uniform stream. In addition to the familiar Kármán vortex street with two vortices per shedding cycle, many complex patterns have been observed, including a mode in which the far-wake region contains three vortices from each shedding cycle. From a large body of literature we mention the studies by Honji & Taneda (1968), Griffin & Ramberg (1974), and Williamson & Roshko (1988), who found that oscillation of a cylinder *normal* to a uniform stream can produce three-vortex patterns. Williamson & Roshko (1988) provide a parameter range over which they found this mode to occur. Griffin & Rambert (1976), Couder & Basdevant (1986), and Ongoren & Rockwell (1988) also observed the three-vortex pattern, but for a cylinder oscillating *in-line* with the uniform stream.

By analogy to the well-known analysis by von Kármán† these observations suggest

† The question arises as to whether a three-dimensional problem can be accurately (and adequately) represented by a two-dimensional model. In this regard we are on more solid ground than von Kármán, for it is well known that a stationary cylinder can shed vortex filaments obliquely, making three-dimensional effects important. However, in the case of an oscillating cylinder, Koopman (1967) and Griffin, Skop & Koopman (1973) have shown that for sufficiently large amplitudes of oscillation ($\geqslant 10\%$ of the cylinder diameter) and appropriate Reynolds numbers the wake becomes essentially two-dimensional.

the following model problem. Consider the (x,y)-plane partitioned into an infinite sequence of strips perpendicular to the x-axis. Let the width of each strip be L. Consider a system of three point vortices placed in one of these strips and periodically continued to all the other strips. Thus, each 'base' vortex corresponds to an infinite row of identical, uniformly spaced vortices, separated one from the next by a distance L. Since the three vortices are to arise from one cycle of a shedding process, we assume in the model that their circulations sum to zero. (This assumption is supported by the observations of Williamson & Roshko 1988.) Of course, the perfect spatial periodicity that we are imposing in the model is not entirely realistic. The experimental situation does not have upstream–downstream symmetry. Nor, to be entirely precise, is an exact periodicity downstream of the cylinder to be expected owing to the influence of the gradually decaying wake 'mean flow'. Similar objections can be raised in the case of von Kármán's model of the vortex street. However, the history of the subject amply shows that his consideration of a point vortex model was worthwhile. We feel that similar comments will be made for the $N = 3$ case once the results of the analysis are assimilated. The problem, then, is to elucidate the motion of this three-vortex problem with the boundary conditions of the periodic strip. As discussed in greater detail below, the problem posed is integrable and can, in principle, be reduced to quadratures. The details of the solution, however, are surprisingly complex.

It is not difficult to show that the dynamics of N point vortices in a periodic strip is given by the equations

$$\frac{\mathrm{d}\bar{z}_\alpha}{\mathrm{d}t} = \frac{1}{2\mathrm{i}L}\sum_{\beta\neq\alpha}\Gamma_\beta \cot\left\{\frac{\pi}{L}(z_\alpha - z_\beta)\right\}. \tag{1.1}$$

In these equations the $z_\alpha = x_\alpha + \mathrm{i}y_\alpha$, $\alpha = 1, \ldots, N$, are complex positions of a set of 'base vortices'. The Γ_β are the circulations of these vortices. The sum is over all base vortices β different from vortex α, the vortex whose velocity is being computed. The overbar on the left-hand side indicates complex conjugation. In the limit $L \to \infty$ these equations reduce to the standard point vortex equations on the unbounded plane. The cotangent interaction between base vortices in (1.1) captures the mutual interactions of each base vortex with the periodic images of all the other base vortices. (The contribution to the velocity of a base vortex from its own periodic images vanishes.)

Although the system (1.1) has been discussed in the literature for many years, its power in addressing problems of vortex rows has not always been appreciated and the literature contains several instances of discovery and re-discovery of solutions to these equations (cf. Aref 1995). The well-known Kármán vortex street arises from $N = 2$ with the conditions $\Gamma_1 + \Gamma_2 = 0$. The common translation velocity of the vortices follows immediately from (1.1) specialized to this case. In this paper our objective is to discuss solutions of (1.1) for the case $N = 3$ under the further condition that

$$\Gamma_1 + \Gamma_2 + \Gamma_3 = 0. \tag{1.2}$$

The problem just outlined has particular theoretical importance in the theory of point vortex dynamics. It has been established that the point vortex equations on the unbounded plane are integrable for $N \leqslant 3$ and *any values* of the circulations (Gröbli 1877; Synge 1949; Novikov 1975; Aref 1979, 1983, 1985; Aref, Rott & Thomann 1992). Integrability comes about due to the existence of certain general integrals of the equations of motion, in particular the *linear impulse*,

$$Q + \mathrm{i}P = \sum_\alpha \Gamma_\alpha z_\alpha \tag{1.3}$$

(where Q and P are the real and imaginary parts, respectively), the *angular impulse*,

$$I = \sum_{\alpha} \Gamma_{\alpha} |z_{\alpha}|^2, \tag{1.4}$$

and the 'Hamiltonian' of the interacting vortices, a quantity related to the kinetic energy of the fluid motion induced by the presence of the vortices. The integrals (1.3) and (1.4) are related to the invariance of the interaction of the vortices on the unbounded plane under continuous spatial symmetries. Thus, Q is conserved owing to translational invariance of the system in the y-direction, P owing to translational invariance in the x-direction, and I is conserved owing to invariance of interactions under rotation of the coordinates.

On the unbounded plane the solution of the three-vortex problem in the general case (where the sum of the circulations is not zero) is based on the integral (1.4) and the Hamiltonian (see the literature just cited). When the sum of the circulations is not zero, the integral (1.3) can in essence be eliminated by a shift of the origin of coordinates. For the special case of vanishing total circulation, however, the solution is most simply based directly on the invariance of Q and P. Details for this case (on the unbounded plane) have been presented by Rott (1989) and Aref (1989). In particular, it was shown that the problem can be 'mapped' onto a problem of advection of a passive particle by three fixed vortices. One may see this reduction as similar to the way the Kepler problem in celestial mechanics of two mass points orbiting one another under the influence of Newtonian gravitation can be mapped onto the motion of a single particle in the gravitational field of a fixed point mass. Professor Rott's suggestion several years ago that the integrable problems of few-vortex systems with zero net circulation would repay more detailed exploration has been an important driving force in our considerations, and has shown itself to be very fruitful.

One might worry that in the periodic strip system only Q, which follows from translational invariance in the y-direction, would survive as an integral. However, as apparently first remarked by Birkhoff & Fisher (1959), P is also conserved in this case. The integral I, of course, cannot be retained. This opens up the possibility of integrating the problem of three vortices in a strip under the special condition (1.2), since the sum of the circulations appears as the Poisson bracket between Q and P, and when this commutator vanishes, Q and P are integrals in involution. These formal points were demonstrated several years ago (Aref 1985), and unpublished numerical experiments by Blomberg (1984) suggested that the system (1.1) for $N = 3$ is chaotic when condition (1.2) is violated. Thus, the particular case that is relevant to the experiments is also – fortunately – precisely the integrable one. Initially, we thought that the solution for this case would be a straightforward extension of the work reported in Rott (1989) and Aref (1989). As we shall see, this is not at all the case. Depending on the actual values of the strengths, the solution to this integrable three-body problem can become very complicated indeed. Some motions that arise appear to us almost counter-intuitive. However, as we shall suggest towards the end of this paper, counterparts of these motions, which play a significant role in the overall dynamics of the problem, appear to arise in the experiments of Williamson & Roshko (1988).

It may be appropriate to mention that the special case of vanishing circulation also plays an important role in the case of *four* point vortices which is, in general, a non-integrable system. Eckhardt & Aref (1988) noted that on the unbounded plane the case $N = 4$, with vanishing total circulation and the additional constraint that $Q = P = 0$, is integrable. A detailed analysis was given by Eckhardt (1989) with two important

postscripts by Rott (1990, 1994). In fact, this case 'maps' onto a three-particle problem that is similar to the general three-vortex problem on the unbounded plane, an observation that we hope to elaborate on elsewhere. In the periodic strip case the modes observed by Williamson & Roshko (1988), in which there are four vortices per cycle, presumably correspond to non-integrable point vortex systems, and would appear to be even more complicated than the three-vortex cases treated in this paper.

We remark that the methods pursued here may be extended to the case of three point vortices in a general periodic parallelogram in the plane (in which case the periodicity assures us that the sum of the circulations is zero). We intend to report on that case, which we believe is relevant to the study of two-dimensional turbulence, in a separate paper.

2. Solution method – preliminary considerations

In order to motivate later considerations, we initially follow the solution path from Aref (1989). We shall see soon enough where it fails us. From (1.2) and (1.3) we find

$$\Gamma_2(z_1-z_2)+\Gamma_3(z_1-z_3) = -(Q+\mathrm{i}P), \tag{2.1a}$$

$$\Gamma_1(z_1-z_2)-\Gamma_3(z_2-z_3) = Q+\mathrm{i}P, \tag{2.1b}$$

so that simple linear relations allow all three vortex separations to be expressed in terms of one, which we take as

$$z_1-z_2 = \zeta. \tag{2.2a}$$

Thus

$$\Gamma_3(z_1-z_3) = -(Q+\mathrm{i}P)-\Gamma_2\zeta, \tag{2.2b}$$

$$\Gamma_3(z_2-z_3) = -(Q+\mathrm{i}P)+\Gamma_1\zeta. \tag{2.2c}$$

Without loss of generality we may assume that the labels of the vortices have been chosen such that $\Gamma_1 \geqslant \Gamma_2 > 0$, $\Gamma_3 < 0$, since two of the vortices must always have the same sign and the case of two negative vortices follows easily from the case of two positive vortices. We set

$$\gamma = \frac{\Gamma_2}{\Gamma_3}+\frac{1}{2}, \tag{2.3a}$$

and then have

$$\frac{\Gamma_1}{\Gamma_3} = -\gamma-\frac{1}{2}, \tag{2.3b}$$

$$\frac{\Gamma_1}{\Gamma_2} = \frac{1+2\gamma}{1-2\gamma}. \tag{2.3c}$$

It follows from these relations that we cover the necessary range of parameters by allowing γ to vary between 0 and $\frac{1}{2}$.

From the equations of motion,

$$\mathrm{d}\bar{z}_1/\mathrm{d}t = -\mathrm{i}\{\Gamma_2 C(z_1-z_2)+\Gamma_3 C(z_1-z_3)\}, \tag{2.4a}$$

$$\mathrm{d}\bar{z}_2/\mathrm{d}t = -\mathrm{i}\{\Gamma_1 C(z_2-z_1)+\Gamma_3 C(z_2-z_3)\}, \tag{2.4b}$$

$$\mathrm{d}\bar{z}_3/\mathrm{d}t = -\mathrm{i}\{\Gamma_1 C(z_3-z_1)+\Gamma_2 C(z_3-z_2)\}, \tag{2.4c}$$

where the abbreviation

$$C(z) = \cot\left\{\frac{\pi}{L}z\right\}\Big/2L, \tag{2.4d}$$

has been used, we obtain an equation for ζ:

$$\frac{\mathrm{d}\bar{\zeta}}{\mathrm{d}t} = \mathrm{i}\Gamma_3[C(\zeta)+C\{X-(\gamma+\tfrac{1}{2})\zeta\}-C\{X-(\gamma-\tfrac{1}{2})\zeta\}], \tag{2.5a}$$

where

$$X = -\frac{Q+\mathrm{i}P}{\Gamma_3}. \tag{2.5b}$$

We comment briefly on the range of the real part of X. We have stressed the notion of 'base vortices' from which an entire row may be constructed by periodic continuation. However, the dynamic problem is invariant to a shift by an integral number of periods within the row of which a vortex is considered the 'base', i.e. simultaneous shifts of z_1, z_2, and z_3 by integral multiples of L in the original setup lead to the same problem. In terms of X, (2.5*b*), this means that changes in its real part by $L\{r(\gamma+\frac{1}{2})-s(\gamma-\frac{1}{2})-t\}$, where r, s and t are integers, lead to the same problem. The smallest positive value that this expression can assume is $(\frac{1}{2}-\gamma)L$. Hence, it is only necessary to vary the real part of X between 0 and $(\frac{1}{2}-\gamma)L$.

The main difference between the periodic strip case and the unbounded plane is now apparent. For the unbounded plane we had equations of the form (2.4), and thus (2.5), but the function C in that case was simply $C(z) = (1/2\pi)z^{-1}$. Hence, quantities such as $C\{X-(\gamma\pm\frac{1}{2})\zeta\}$ could be rewritten in the form $AC(\zeta-B)$ with suitably chosen constants A and B. This allowed the right-hand side of the counterpart of (2.5*a*) (see (A 6) of Aref 1989) to be interpreted immediately as an advection problem for a passive particle in the field of three fixed vortices. For the case at hand such an interpretation is more elusive.

In the next section we consider the special case $\gamma = 0$ ($\Gamma_1 = \Gamma_2$). Based on insight derived from that case we present in §4 a general solution method for any rational value of γ. An interpretation of the motion in terms of an advection problem by a system of fixed vortices in a wider periodic strip is possible in this case. Depending on the width of the strip and the number of fixed vortices in it, that advection problem may become quite complicated. Representative examples are given in §5, concentrating on the case $\Gamma_1:\Gamma_2:\Gamma_3 = 2:1:(-3)$, which seems to capture the essential regimes of motion that we have observed for other rational values of γ, but that do not arise for $\gamma = 0$. In §§4 and 5 we also discuss the bifurcations of the streamline patterns produced by the fixed vortices as X, (2.5*b*), is varied. In §6 we explain how the reduction to an advection problem by fixed vortices may be obtained for an arbitrary real value of γ. The advection problem now does not 'fit' into a periodic strip but involves three infinite rows of fixed vortices. We also comment on the issue of 'convergence' of a series of periodic advection problems corresponding to rational approximants of an irrational γ to the infinite row case corresponding to γ itself. Finally, in §7 we return to the results of Williamson & Roshko (1988) and argue that, indeed, a counterpart of one of the dominant modes of motion found in the analysis of §§4 and 5 appears to occur in the experiments.

3. The special case $\gamma = 0$ ($\Gamma_1 = \Gamma_2$)

The equation to be solved in this case is

$$\frac{\mathrm{d}\bar{\zeta}}{\mathrm{d}t} = \mathrm{i}\Gamma_3[C(\zeta)+C\{X-\tfrac{1}{2}\zeta\}-C\{X+\tfrac{1}{2}\zeta\}]. \tag{3.1}$$

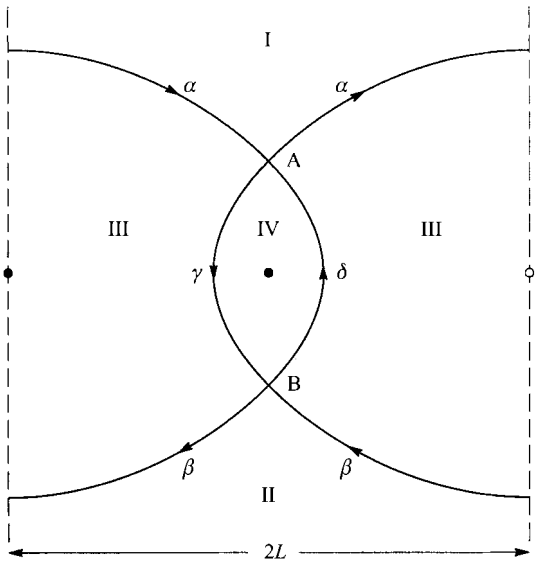

FIGURE 1. Phase space for $\Gamma_1:\Gamma_2:\Gamma_3 = 1:1:(-2)$, $\gamma = 0$, and $X = 0$. The strip width is $2L$ and there are two advecting vortices (solid dots). The four regimes of motion are labelled I–IV, the saddle points are A and B, and the separatrices are designated α, β, γ and δ.

In order to interpret this as an advection problem by fixed vortices (in a periodic strip) we note the identity

$$2\cot\left(\frac{\pi}{L}\zeta\right) = \cot\left\{\frac{\pi}{2L}\zeta\right\} + \cot\left\{\frac{\pi}{2L}(\zeta - L)\right\}. \tag{3.2}$$

Thus, (3.1) may be rewritten

$$\frac{\mathrm{d}\bar{\zeta}}{\mathrm{d}t} = \mathrm{i}\Gamma_3[c(\zeta) + c(\zeta - L) - 2c(\zeta - 2X) - 2c(\zeta + 2X)], \tag{3.3a}$$

where

$$c(z) = \cot\left\{\frac{\pi}{2L}z\right\}\Big/4L. \tag{3.3b}$$

This equation has an immediate interpretation as an advection problem for a passive particle in the field of *four* fixed vortices, two of strength $-\Gamma_3$, two of strength $2\Gamma_3$, in a periodic strip of width $2L$. The two vortices of strength $-\Gamma_3$ are located at $z = 0$ and $z = L$. The two vortices of strength $2\Gamma_3$ are located at $\pm 2X \pmod{2L}$. Note that the strengths of the fixed vortices do not sum to zero.

A particularly simple case arises if $X = 0$. Then there are just two fixed, advecting vortices, one of strength $3\Gamma_3$ at $z = 0$ and one of strength $-\Gamma_3$ at $z = L$ in the strip of width $2L$. The pattern of particle paths (or, equivalently, streamlines) in the steady flow produced by these fixed vortices is shown in figure 1. All streamlines shown are separatrices or 'dividing streamlines', i.e. they connect stagnation points of the advection problem. There are four regimes of motion, labelled I, II, III and IV in figure 1. Here and subsequently, regimes of motion are designated by Roman numerals, motions along separatrices by lower-case Greek letters, and stagnation (saddle) points by upper-case English letters. The motion is bounded, in the sense that $|\zeta|$ is bounded, in regimes III and IV, unbounded in regimes I and II. According to (2.2*a*) this means

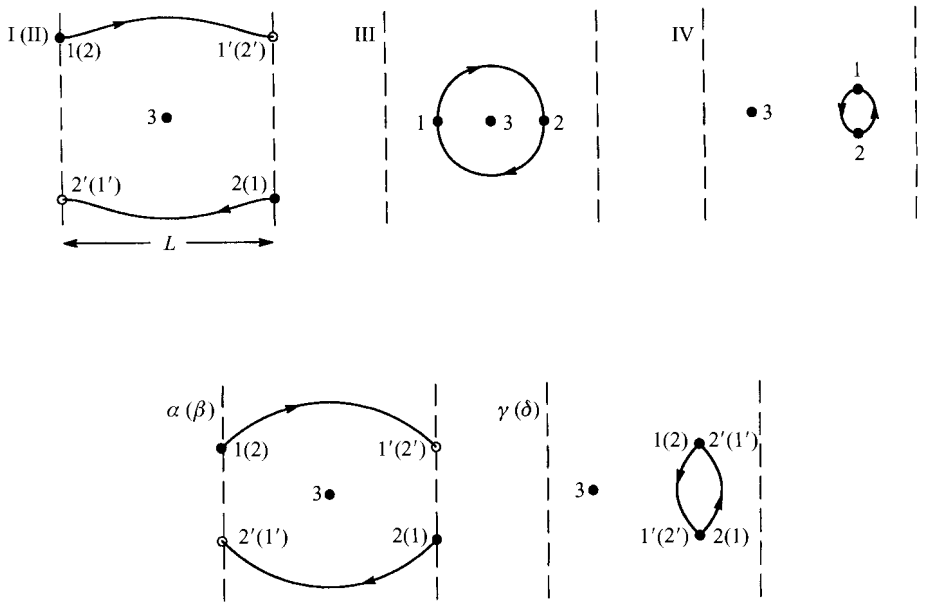

FIGURE 2. Real-space trajectories of the three vortices corresponding to the phase-space diagram of figure 1. Base vortices are shown as solid circles, periodic images as open circles. Vortex 3 is stationary in all cases. Initial positions are labelled 1, 2; final positions 1′, 2′. All motions are shown for one period (in the case of separatrices: for the transition from saddle to saddle). The motion in II, β, and δ are obtained by interchanging vortices 1 and 2 in I, α, and γ, respectively.

that the corresponding trajectories of the three vortices in 'real space' are such that vortices 1 and 2 stay together in regimes III and IV, whereas they separate in regimes I and II. According to (2.2*b*) and (2.2*c*) when vortices 1 and 2 separate, all three vortices will separate, i.e. although they start in the same periodic strip, they will over time migrate farther and farther away so that these base vortices are eventually separated by many strips. There are, of course, periodic images in each strip, but the effect remains that considerable interchange or 'mixing' occurs along the rows in this case compared to cases when the base vortices remain within one or two strips of each other for all time. The top three panels in figure 2 display typical trajectories of the base vortices for each of the four regimes in figure 1 according to the labels indicated. Note that in this case the condition $X = 0$ means $z_3 - z_1 = -(z_3 - z_2)$, so (2.4*c*) shows that z_3 is constant, i.e. vortex 3 remains stationary. The conventions used in figure 2 (and later in other trajectory plots) are that the original base vortices are indicated by solid circles. Their initial positions are given by the numbers 1, 2 and 3; the final positions by 1′, 2′ (and 3′ when it moves). Motion in regime II looks exactly like motion in regime I except that the numbering of vortices 1 and 2 is interchanged (and so indicated in parentheses in figure 2). The bottom two panels of figure 2 correspond to the separatrices α, β and γ, δ in figure 1, respectively.

The very simple picture that emerges for $X = 0$ is immediately complicated when $X \neq 0$. Figure 3, for example, shows the result of the same construction for $X = L(1+\mathrm{i})/8$. Now we encounter all four fixed, advecting vortices (in a strip of width $2L$), and so to the simple picture of regimes I–IV in figure 1 we must add regimes V, VI and VII to accommodate the two additional vortices. The dividing streamlines of the flow produced by the fixed vortices are as shown in figure 3. It is clear that all advected particle trajectories are closed in the sense that they either close on themselves or on their periodic image in the next strip of width $2L$. Hence, all real-space motions of the

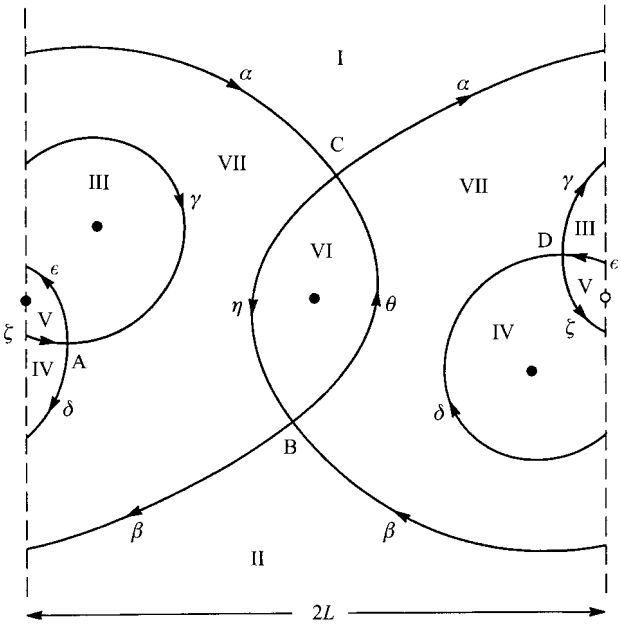

FIGURE 3. Phase space for $\Gamma_1:\Gamma_2:\Gamma_3 = 1:1:(-2)$, $\gamma = 0$, and a 'generic' value of $X = L(1+i)/8$. The strip width is $2L$ and there are now four advecting vortices (solid dots). The regimes of motion are labelled I–VII, the saddle points are A–D, and the separatrices are designated by small Greek letters.

original three vortices (except for the 'separatrix' motions corresponding to the dividing streamlines themselves) are periodic, and the initial configuration reassembles itself after some time, possibly modulo a number of periodic strips, i.e. in order to reassemble the original configuration we may need to employ the periodic image of one or more base vortices. Figure 4 provides sample trajectories of motions in the various regimes of figure 3 as indicated by the labels. The conventions used in figure 4 are again that the original base vortices are indicated by solid circles. Their initial positions are given by the numbers, 1, 2 and 3; the final positions by 1′, 2′, 3′. In the initial and final configurations we also join three vortices by lines to form a triangle to more clearly illustrate how the vortex configuration re-emerges after a period (or how a steady state at one end of a separatrix arises from the steady state at the other end). In some cases (e.g. I, II and α, β) the motion of periodic images is essential in order to understand how this re-emergence comes about. In these cases the required periodic images and their initial and final positions are indicated by open circles and numbering 2″, 3″ for the final positions. The trajectories of periodic images are given by lighter lines than the trajectories of the base vortex trio.

Note that in regime I (II) the re-assembly of the initial configuration arises by vortex 1 (2) 'teaming up' with periodic images of vortices 2 (1) and 3. In the other regimes the vortices from one strip 'travel together' and re-assemble the initial configuration at some shifted position. The four bottom panels in figure 4 show separatrix motions as labelled in figure 3. It can be seen here that the separatrices really tell much of the story in the sense that the motion in any one of the regimes resembles the motion along the separatrices bounding that regime. For example, the motion in the panel labelled III in figure 4 is a 'mixture' of the separatrix motions labelled γ and ϵ, as would be expected from figure 3. Similarly, the motion in regime I (II) follows quite closely the motion corresponding to the separatrix α (β). This idea, that the general motion can be understood on the basis of the separatrix motions in the advection problem, will be

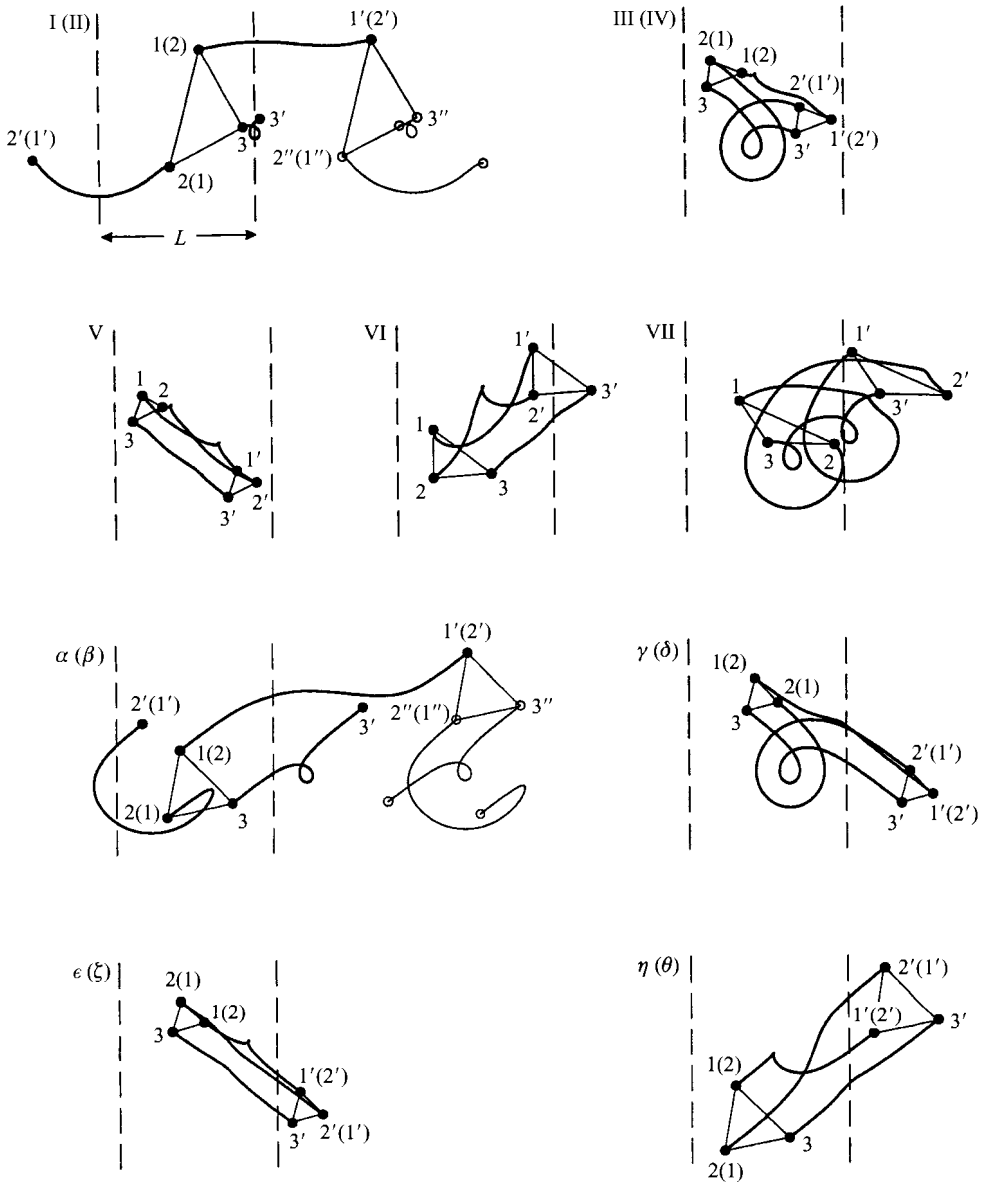

FIGURE 4. Real-space trajectories of the three vortices corresponding to the phase-space diagram of figure 3. Base vortices are shown as solid circles and their trajectories as heavier lines; periodic images are open circles and their trajectories are lighter lines. Initial positions are labelled 1, 2, 3; final positions 1′, 2′, 3′. Final positions of required periodic images are labelled 1″, 2″, 3″. The trajectories are labelled according to the regimes and separatrices indicated in figure 3. All motions are shown for one period (in the case of separatrices: for the transition from saddle to saddle). Note that since vortices 1 and 2 may be interchanged, regimes and separatrices pairwise may lead to similar real-space trajectories. The motion in II, IV, β, δ, ζ, and θ is obtained by interchanging vortices 1 and 2 in I, II, α, γ, ϵ, and η, respectively.

utilized as we proceed. Note, however, that the motions within regimes are strictly periodic, whereas the separatrix motions begin and end infinitesimally close to an unstable steady state. Hence, the extent (in real space) of a separatrix motion as displayed in our figures is somewhat arbitrary, since it can be continued 'forever' both

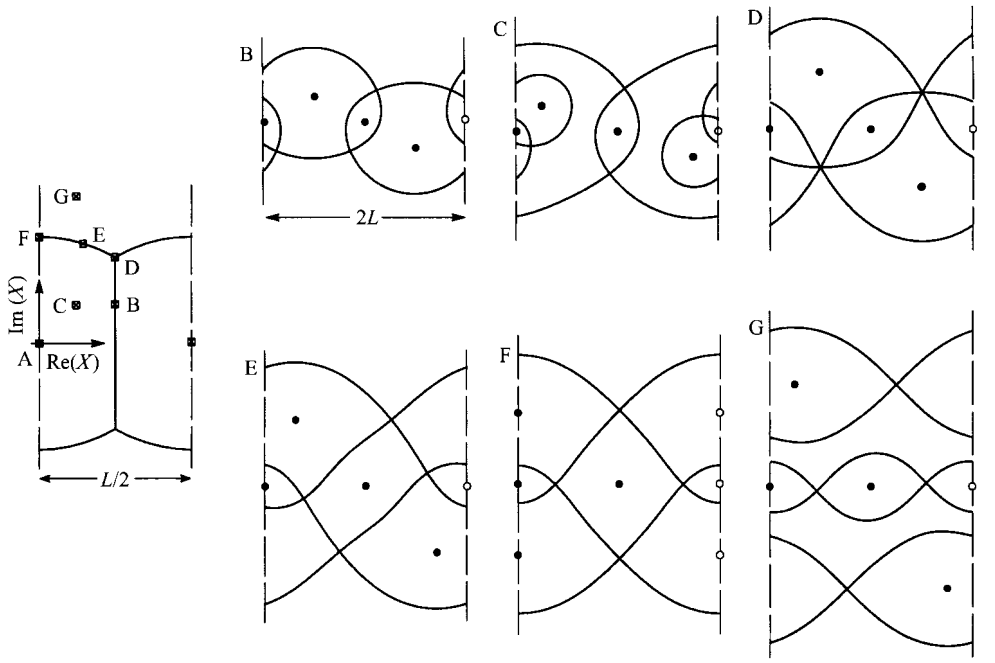

FIGURE 5. Bifurcation diagram in X-space and representative streamline patterns in the field of the fixed vortices. The streamline pattern corresponding to A is figure 1. The streamline pattern C is figure 3. Streamline pattern G is reproduced in greater detail in figure 6.

before and after the segment shown, whereas the trajectory plots within regimes are true, single-period motions.

A complete discussion of the variability of a streamline pattern such as figure 3 with X leads us to a bifurcation analysis, the results of which are indicated in figure 5. On the left we show a bifurcation diagram in the X-plane, with the real part of X restricted to the interval from 0 to $L/2$ as discussed in §2. For this case, i.e. for $\gamma = 0$, bifurcations in the streamline topology of the advection problem, such as figures 1 and 3, occur only along the curves indicated in figure 5 (left panel). For example, point A in this bifurcation diagram corresponds to $X = 0$ and leads to figure 1 with four regimes of motion. If we increase both the real and imaginary parts of X, we arrive at point C in the bifurcation diagram, and we see from the small panel C in the right-hand part of figure 5 that the streamline pattern from figure 3, with seven regimes of motion, has been achieved. When the real part of X is $L/4$, there is a range of imaginary parts of X for which the streamline pattern has the topology indicated in figure 5(B). This streamline pattern leads to six regimes of motion. As the imaginary part of X is increased, we eventually reach point D in the bifurcation diagram with a streamline pattern as shown in panel D of figure 5. The 'accidental degeneracy' of saddle points is evident (and the three streamlines passing through the two stagnation points produce six sectors of opening angle $\pi/3$). Varying X along the upper curve DEF in the bifurcation diagram produces streamline patterns E and F. (D, E and F all have six regimes of motion.) Finally, for large imaginary parts of X, i.e. for large values of the impulse in the x-direction, we find streamline patterns such as G with eight regimes of motion.

We have explored the nature of the motions of the original three vortices arising from the various regimes seen in figure 5(B–G). The only substantial addition to what we saw in our discussion of figures 3 and 4 are the motions, shown in figure 6,

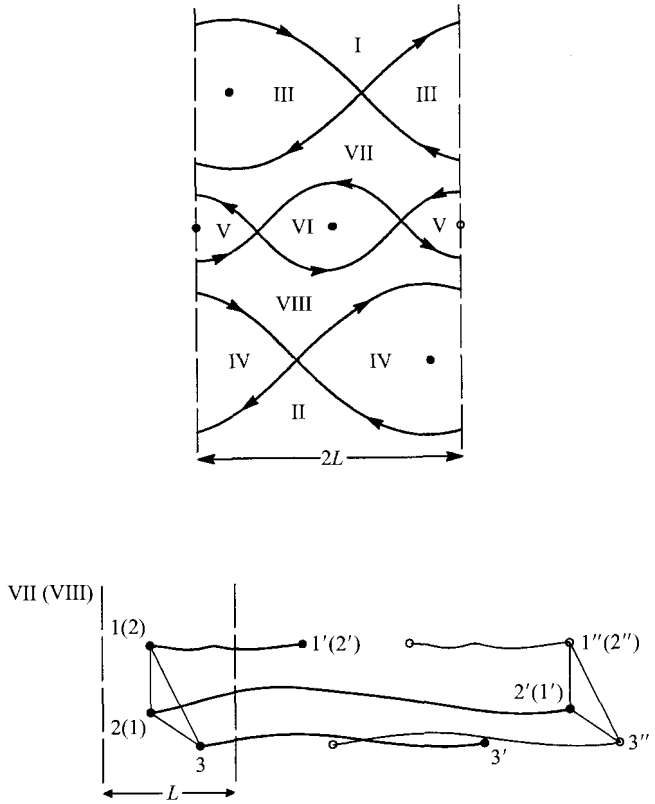

FIGURE 6. Streamline pattern G from figure 5 (top) and representative vortex trajectories corresponding to regimes VII and VIII (bottom).

corresponding to the regimes from panel G in figure 5 (reproduced at the top of figure 6) labelled VII and VIII. Sample vortex trajectories are shown at the bottom of figure 6. We find a new type of motion, which strongly involves periodic images from adjacent strips. Although superficially similar to the motions in regimes I and II of figure 3, the base vortices now all move in the same direction. The motions corresponding to regimes I–VI in figure 6 are qualitatively similar to those motions with the same Roman numerals discussed in figures 3 and 4.

4. Solution method for rational γ

We may base a general approach for the case of rational γ on a generalization of (3.2). Let us consider a periodic row of identical vortices of strength Γ with spacing L. Assume coordinates are chosen such that the vortices are at $x = 0, L, 2L, \ldots$, etc. Let us now calculate the induced velocity from this row of vortices on an advected particle at z. First, view the row as a single vortex placed in a strip of width L repeated infinitely in both directions. Then the (complex conjugate of the) velocity in question is simply $(\Gamma/2Li)\cot(\pi z/L)$. Next, view the row as consisting of N identical vortices placed at $x = 0, L, 2L, \ldots, (N-1)L$ in a periodic strip of width NL. Then the velocity is given as a sum of N cot terms. Equating the two expressions we have

$$\frac{\Gamma}{2Li}\cot\left(\frac{\pi}{L}z\right) = \frac{\Gamma}{2NLi}\sum_{n=0}^{N-1}\cot\left\{\frac{\pi}{NL}(z-nL)\right\}, \tag{4.1a}$$

or
$$\cot\left(\frac{\pi}{L}z\right) = \frac{1}{N}\sum_{n=0}^{N-1}\cot\left\{\frac{\pi}{NL}(z-nL)\right\}. \tag{4.1b}$$

Introducing the notation
$$c_r(z) = \cot\left(\frac{\pi}{rL}z\right)\Big/2rL \tag{4.2}$$

(such that $C(z)$ in (2.4d) corresponds to $r = 1$ and $C(z)$ in (3.3b) corresponds to $r = 2$) we may write this as
$$c_1(z) = \sum_{n=0}^{N-1} c_N(z-nL). \tag{4.3}$$

Note also that
$$rc_r(rz) = c_1(z). \tag{4.4}$$

We now return to (2.5a) and assume that γ is a rational number written in lowest terms as p/q, where p and q are integers with $q > 2p$ (since $\gamma < \frac{1}{2}$). Using (4.3) and (4.4) we rewrite the second term on the right-hand side of (2.5a) as follows:
$$C\{X-(\gamma+\tfrac{1}{2})\zeta\} = -c_1\left(\frac{q+2p}{2q}\zeta - X\right) = -\sum_{n=0}^{q+2p-1} c_{q+2p}\left(\frac{q+2p}{2q}\zeta - X - nL\right)$$
$$= \frac{-1}{q+2p}\sum_{n=0}^{q+2p-1} c_1\left(\frac{\zeta}{2q} - \frac{X+nL}{q+2p}\right) = \frac{-2q}{q+2p}\sum_{n=0}^{q+2p-1} c_{2q}\left\{\zeta - \frac{2q(X+nL)}{q+2p}\right\}. \tag{4.5a}$$

Similarly,
$$C\{X-(\gamma-\tfrac{1}{2})\zeta\} = \frac{2q}{q-2p}\sum_{n=0}^{q-2p-1} c_{2q}\left\{\zeta + \frac{2q(X-nL)}{q-2p}\right\}; \tag{4.5b}$$
$$C(\zeta) = \sum_{n=0}^{2q-1} c_{2q}(\zeta - nL). \tag{4.5c}$$

Thus, all three terms on the right-hand side of (2.5a) have been rewritten in terms of velocities induced by a system of fixed vortices of various strengths in a periodic strip of width $2qL$. The total number of fixed vortices is $q+2p+(q-2p)+2q = 4q$. The differential equation for ζ, which now reads
$$\frac{d\bar{\zeta}}{dt} = i\Gamma_3\left[\sum_{n=0}^{2q-1} c_{2q}(\zeta - nL) - \frac{2q}{q+2p}\sum_{n=0}^{q+2p-1} c_{2q}\left\{\zeta - \frac{2q(X+nL)}{q+2p}\right\}\right.$$
$$\left. - \frac{2q}{q-2p}\sum_{n=0}^{q-2p-1} c_{2q}\left\{\zeta + \frac{2q(X-nL)}{q-2p}\right\}\right], \tag{4.6}$$

may be interpreted as a problem of passive advection of a particle in the velocity field produced by these fixed vortices. The special case considered in §3 corresponds to $q = 1$ (and $p = 0$).

For a given $\gamma = p/q$ we are thus instructed by (4.6) to consider the advection of a particle by a system of fixed vortices in a periodic strip of width $2qL$. There are three families of vortices. At the $2q$ locations $0, L, \ldots, (2q-1)L$ we find identical vortices of circulation $-\Gamma_3$. The locations of the two other families of vortices depend on the value of the impulse in the original problem, here represented by the quantity X. The $q+2p$ vortices located at $2q(X+nL)/(q+2p) = -(\Gamma_3/\Gamma_1)(X+nL)$, $n = 1, \ldots, q+2p-1$ all have circulation $2q\Gamma_3/(q+2p) = -\Gamma_3^2/\Gamma_1$; the $q-2p$ vortices at

$2q(-X+nL)/(q-2p) = -(\Gamma_3/\Gamma_2)(-X+nL)$, $n = 1, \ldots, q-2p-1$ all have circulation $2q\Gamma_3/(q-2p) = -\Gamma_3^2/\Gamma_2$. (The reader of Rott 1989 and Aref 1989 should recognize these circulation values!) Note that although the sum of the original three vortex circulations vanishes, the net strength of the fixed vortices in the advection problem for ζ is $2q\Gamma_3$ ($\neq 0$). When X is real all three families of vortices are situated on the real axis and, depending on the values of p and q, vortices from the different families may coincide (in which case a single vortex is placed with a circulation equal to the sum of the circulations of the coinciding vortices). When X has a non-vanishing imaginary part, the three families of vortices are always distinct: one family remains on the real axis, the second will be situated above it and the third below it. Changes in the topology of the streamlines governing the advection problem lead to a bifurcation problem with X as the bifurcation parameter. We have seen an example of this in figure 5, and we will show and discuss another, more complicated example in figure 8.

The motion of a passively advected particle in the flow field induced by these three rows of fixed vortices can be used, via (2.2*a–c*), to construct and classify the trajectories of the original three vortices in the periodic strip. For brevity and clarity we shall refer to the trajectories of the original vortices as the vortex motion in 'real space'. We shall refer to the advection problem as the motion in 'phase space'.

In general we expect the phase space to be a periodic strip of width $2qL$. From the considerations just given we may, however, derive sharper results. Without loss of generality consider a shift of the base vortices in which base vortex 1 is shifted by rL, base vortex 2 by sL and base vortex 3 is not shifted at all. This changes ζ by $(r-s)L$. In order to be considering an equivalent problem, we must assure that X is not changed, i.e. r and s must satisfy $r(\gamma+\frac{1}{2}) = s(\gamma-\frac{1}{2})$. With $\gamma = p/q$ this mean $2p(s-r) = q(s+r)$. We are only interested in $q > 2$. Consider first the case where q is odd. Since p and q are relatively prime, this relation tells us that $s+r$ must be a multiple of p and $s-r$ must be a multiple of q, i.e. there must exist an integer k such that $s-r = kq$, $s+r = 2kp$. Solving for r and s we have $2s = k(2p+q)$, $2r = k(2p-q)$. Since q is odd, it follows from these that k must be even. The smallest shift in ζ that leads to an equivalent problem thus occurs for $k = 2$, and is $2qL$. Thus, the phase space will be periodic with period $2qL$ for odd q and we should not expect a shorter period. For even q the situation is different. We set $q = 2u$ and note that p must now be odd. The equation $2p(s-r) = q(s+r)$ becomes $p(s-r) = u(s+r)$, where u and p are relatively prime. There then exists a k such that $s-r = ku$, $s+r = kp$, and $2s = k(p+u)$, $2r = k(p-u)$. Now, if u is odd, $p+u$ is even, and $k = 1$ gives the smallest value of $s-r$, namely $(q/2)L$. On the other hand, if u is even, k must also be even, the smallest value of $s-r$ occurs for $k = 2$, and is qL. Thus, for even q the phase space will already be periodic with period qL if q is divisible by 4, and with period $(q/2)L$ if q is not divisible by 4. The latter period is four times shorter than the general result $2qL$ would have led us to believe. The case $(p, q) = (1, 6)$, corresponding to circulations $\Gamma_1:\Gamma_2:\Gamma_3 = 2:1:(-3)$, is the simplest example of a phase space with such a shorter period. This case will be studied in detail in §5.

It is not difficult to verify, as we have already remarked, that the coincidence of ζ with one of the vortices in the phase space corresponds to the coincidence of two of the original vortices 1, 2, and 3 in real space (modulo L). For example, if $\zeta = 2q(X+nL)/(q+2p)$, then $z_2 - z_3 = X - (\gamma+\frac{1}{2})\zeta = -nL$. This is, of course, not allowed. However, it is useful to note that ζ-motion in the vicinity of a phase-space vortex in the row with positions $2q(X+nL)/(q+2p)$ corresponds to real-space motion in which vortices 2 and 3 'move as a pair'. Similarly, ζ-motion in the vicinity of a phase-space vortex in the row with positions nL corresponds to real-space motion in which vortices

1 and 2 'move as a pair', and ζ-motion in the vicinity of a vortex in the row with positions $2q(-X+nL)/(q-2p)$ corresponds to real-space motion in which vortices 1 and 3 'move as a pair'. We should recall that the notion of 'moving as a pair' can lead to rather different patterns of motion depending on both the relative sign and magnitude of the circulations of the two vortices in the pair.

5. Representative examples

Among the simplest rational values of γ to consider are $(p, q) = (1, 3)$, $(1, 5)$ and $(2, 5)$ corresponding to the vortex strength ratios $\Gamma_1:\Gamma_2:\Gamma_3 = 5:1:(-6)$; $7:3:(-10)$; and $9:1(-10)$, respectively. In all these cases q is odd and the phase-space periodic strip is of width $2qL$. The phase-space diagram for the case $(p, q) = (1, 6)$, where q is even but not divisible by 4, fits in a strip of width $3L$. The corresponding vortex strengths, $\Gamma_1:\Gamma_2:\Gamma_3 = 2:1:(-3)$, probably give the simplest set to consider after the case $\gamma = 0$ of §3. On one hand, the phase-space diagram for this case reveals regimes of motion that are not present for $\gamma = 0$. On the other hand, it seems to capture the phase-space structures that appear for other rational values of γ that we have explored. Hence, we begin our study of specific examples by an analysis of the motion in the case $(p, q) = (1, 6)$, and then briefly show how the regimes of motion found for this case have counterparts in more complex motions corresponding to $(p, q) = (1, 5)$ and $(2, 5)$. We have considered other examples as well, such as $(p, q) = (1, 3)$, $(1, 7)$, $(2, 7)$, and so on, but we have not found regimes of motion qualitatively different from the examples selected for presentation below.

Figure 7 shows phase-space streamlines for $(p, q) = (1, 6)$, and $X = L(1+3i)/12$. All streamlines shown are separatrices or 'dividing streamlines', i.e. they connect stagnation points of the phase-space advection problem, in a strip of width $3L$. The chosen value of X is generic in the sense that the streamline pattern does not display any symmetries that may arise for other, more carefully chosen, values of X. The bifurcation diagram in X-space, i.e. the analogue for this problem of figure 5, is quite complicated. We show it in the left panel of figure 8. Four representative streamline patterns are shown in panels A, B, D and E in the right-hand portion of figure 8. They correspond to the X-values indicated as A, B, D and E in the bifurcation diagram. Of these four, A and D are on curves of the bifurcation diagram and thus have some 'degeneracy' or symmetry, in the sense that two or more saddle points in the phase-space streamline pattern are connected at the corresponding values of X. The X-value marked C in figure 8 leads to the streamline pattern in figure 7 that will be analysed in detail.

It is important to note that the approximate dipole structures seen in figures 7 and 8, e.g. in figure 7 the one with regions labelled IV and VIII and saddle points labelled D and E, are essential features of these patterns, and are the main new feature (arising from $\gamma \neq 0$) relative to figures 1 and 3. At first sight one might think it an error that there is not a single separatrix curve connecting D to E. However, this kind of connection does not arise, and if one traces the separatrices (which is not entirely simple since several of them are very close), one finds that both D and E are connected up to themselves by two loops, i.e. the pattern of separatrices is topologically like a 'figure 8' with D or E at the cross. These dipole-like structures around a pair of fixed vortices are quite different from the more familiar connected configurations that arise in such problems as the 'atmosphere' of a translating vortex pair. The streamline topologies in figures 7 and 8 are, in general, of this 'disconnected' type, and the bifurcation diagram in figure 8 arises precisely from a careful tracing of when saddle

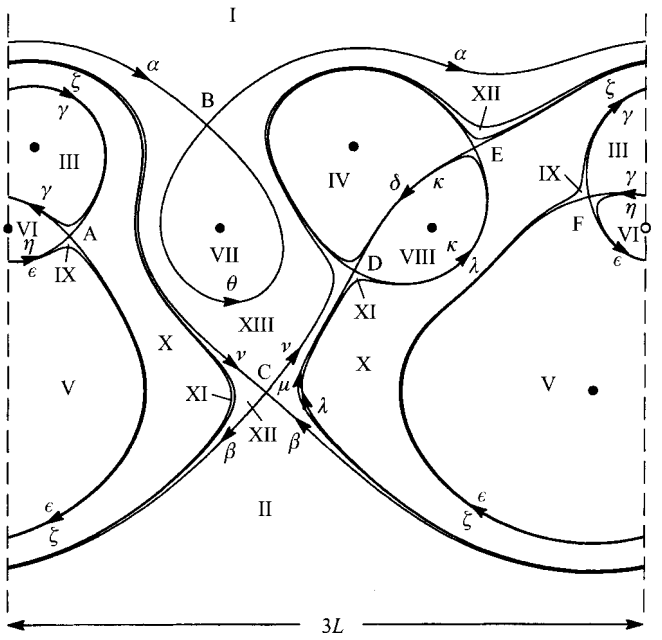

FIGURE 7. Phase space for $\Gamma_1:\Gamma_2:\Gamma_3 = 2:1:(-3)$, $\gamma = 1/6$, and a 'generic' value of $X = L(1+3i)/12$. The strip width is $3L$ and there are 6 advecting vortices (solid dots). The regimes of motion are labelled I–XIII, the saddle points are A–F, and the separatrices are designated by small Greek letters. Note the lack of connection between saddle points such as D and E that 'belong' to the same dipole-like structure. Note also the very thin regimes of motion, such as IX, XI and XII.

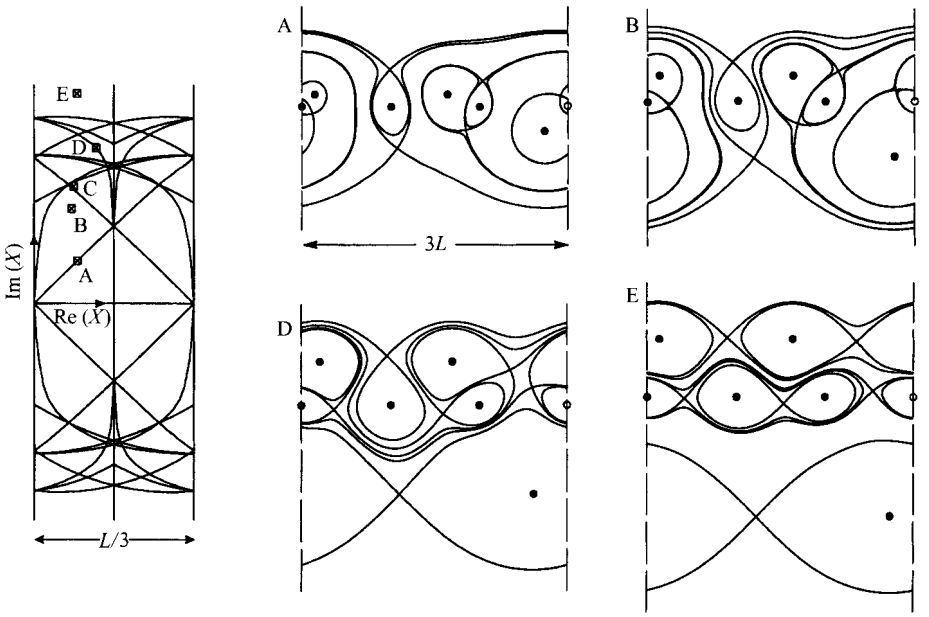

FIGURE 8. Bifurcation diagram in X-space (left) for the case of $\Gamma_1:\Gamma_2:\Gamma_3 = 2:1:(-3)$, $\gamma = 1/6$. The value of X indicated as C corresponds to the streamline pattern in figure 7. The streamline patterns corresponding to values of X indicated as A, B, D and E are shown at right.

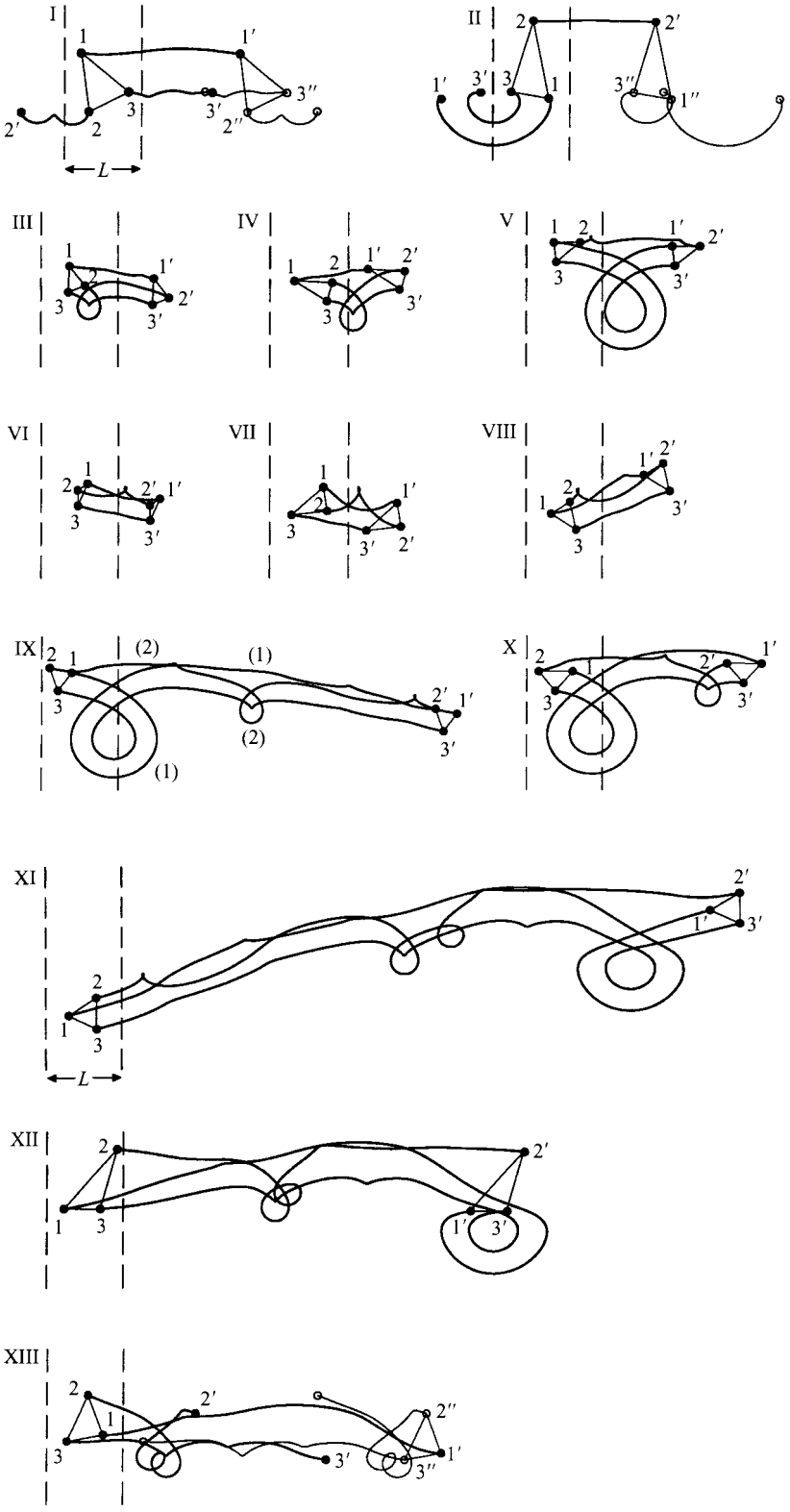

FIGURE 9. For caption see facing page.

points connect. In general, if one computes to high accuracy the values of the streamfunction at the two saddle points (such as D and E in figure 7) on either side of an apparent dipole, one finds them to differ by a few percent. On the other hand, at a bifurcation the values of the streamfunction at two apparently connected saddle points agree to all significant digits (and this is how the bifurcation diagram is determined). The existence of these 'disconnected' dipole streamline patterns leads to regimes of motion that reside in very thin strips of phase space (e.g. the regions marked IX, XI, and XII in figure 7) yet are clearly identifiable in the real-space dynamics of the vortices. A diagram such as figure 7 thus has as many as 13 distinct regimes of motion! We have once again labelled these by Roman numerals. In figure 9 we show representative real-space vortex trajectories (of the base vortices) corresponding to these various regimes. The richness of some of these motions, all of which are periodic, is remarkable. Note in particular the complexity of the motions associated with the aforementioned 'thin strips' in phase space (see, for example, the trajectory plot labelled XI in figure 9).

The general nature of each of the trajectory plots in figure 9 can be understood by reference to figure 7 and use of the formulae (2.2*a–c*). We have already commented on the nature of real-space trajectories when ζ orbits one of the fixed phase-space vortices. Examples are shown in panels III, IV, V, VI, VII, and VIII of figure 9. More interesting, and certainly more pervasive in the phase-space plot of figure 7, are the regimes that pass by several of the fixed vortices. Trajectory examples are shown in panels I, II, IX, X, XI, XII and XIII of figure 9. Both bounded and unbounded motions occur in the sense that the original base vortices stay together or separate indefinitely. Bounded motion occurs in regimes IX, X, XI and XII; unbounded motion in regimes I, II and XIII. Clearly, the number of periodic strips that separate the final and initial positions of the base vortices, and whether the re-emergence of the original pattern involves periodic image vortices or not, has significant consequences for such processes as mixing. Some of the trajectories (e.g. XI) are quite complex with the vortices moving through very complicated turns, some of them very sharp. We stress that all motions are periodic, and that the complexity seen in figure 9, e.g. that the vortices travel several periodic strip widths before rearranging into the original pattern, is all happening in periodic motions. We also stress the appearance and prevalence of motions such as I and II, since we believe them to be among the ones observed experimentally, as we discuss in §7.

The separatrix motions that connect different steady-state 'vortex streets' clearly provide a key to understanding the entire diagram. We have calculated the real-space motion corresponding to the various separtrices in figure 7, and these are presented in figure 10. Knowing the separatrix motions in real space and knowing the phase space it is possible to develop a qualitative picture of any real-space motion by piecing together the appropriate separatrix motions. Thus, a trajectory such as XI in figure 9 is clearly made up of pieces that resemble separatrices κ and μ, i.e. the two 'loops' that share saddle point D in figure 7.

An interesting corollary of all these developments is that *there are no stable steady configurations*. Steady configurations of the three vortices in real space correspond to

FIGURE 9. Real-space trajectories of the three vortices corresponding to regimes I–XIII in the phase-space diagram of figure 7. Base vortices are shown as solid circles and their trajectories as heavier lines; periodic images are open circles and their trajectories are lighter lines. The trajectories are labelled according to the regimes indicated in figure 7. Initial positions are labelled 1, 2, 3; final positions 1′, 2′, 3′. Final positions of required periodic images are labelled 1″, 2″, 3″. All motions are shown for one period.

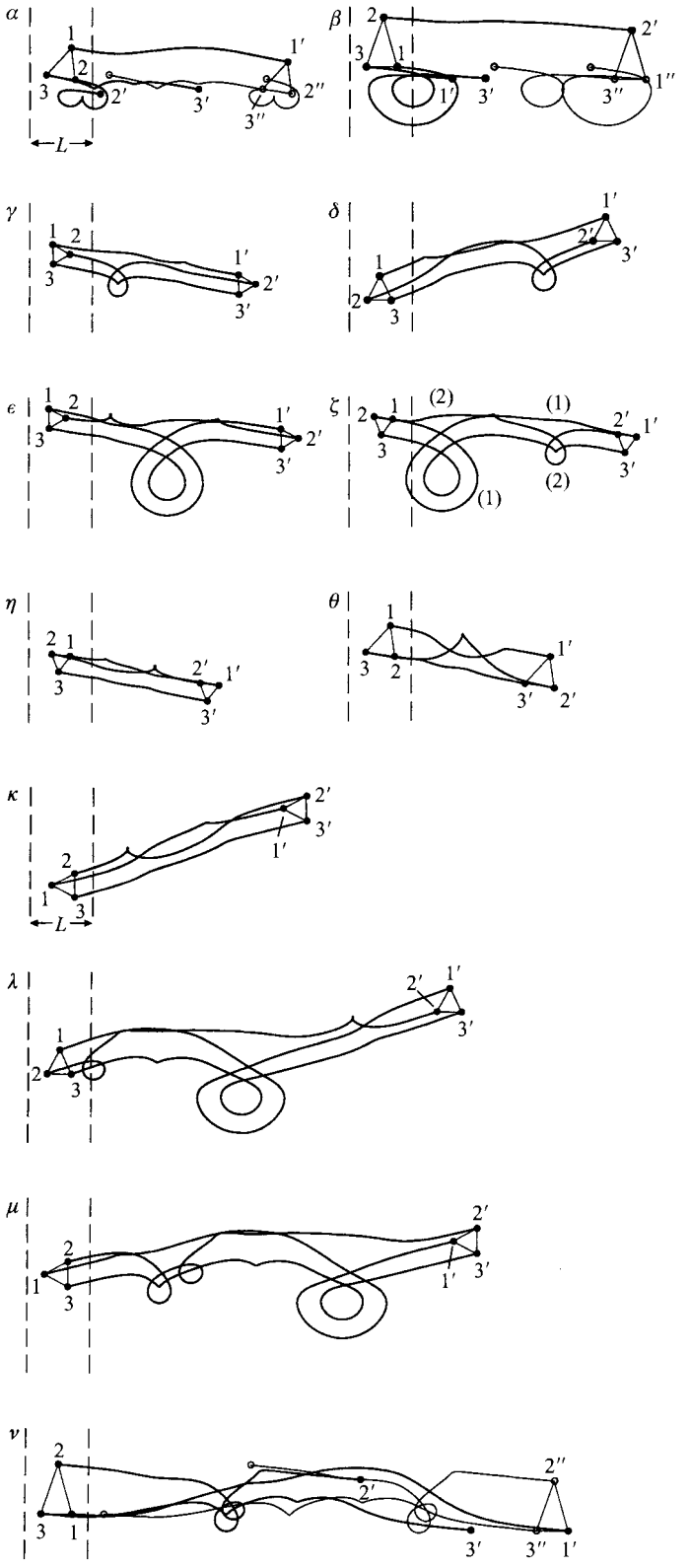

FIGURE 10. For caption see facing page.

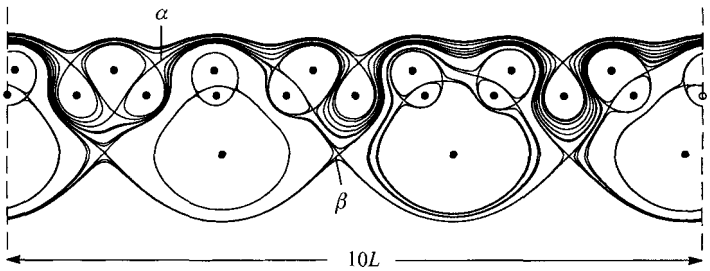

FIGURE 11. Phase space for $\Gamma_1:\Gamma_2:\Gamma_3 = 7:3:(-10)$, $\gamma = 1/5$, and $X = L(3+10i)/40$. The strip width is $10L$ and there are 20 advecting vortices (solid dots). Two separatrices are labelled (cf. figure 12).

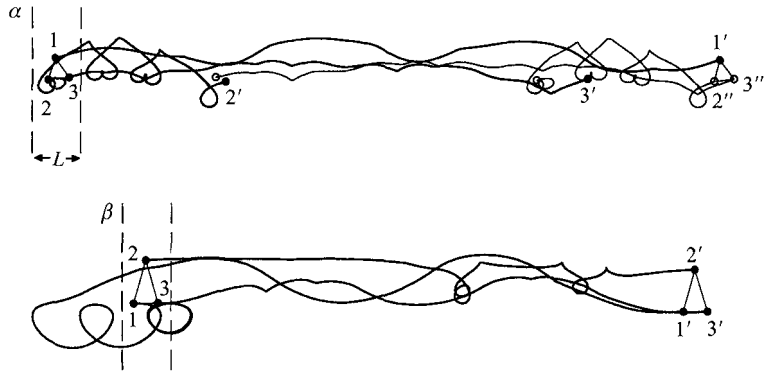

FIGURE 12. Real-space trajectories of the three vortices corresponding to the two separatrices α and β in the phase-space diagram of figure 11. Notation as in figure 9. All motions are shown for the transition from saddle to saddle.

stagnation points of the advecting flow in phase space. These come in two varieties: there are the locations of the advecting vortices, and there are a number of hyperbolic points in the flow field away from the vortices. There cannot be elliptic points in the flow field since it is a potential flow induced by a fixed set of point vortices. Clearly, the real-space state corresponding to any hyperbolic point is not stable, since there exist perturbations that will amplify exponentially. And, as we have already seen, the advecting point vortices correspond to real-space states in which two vortices are at the same location, i.e. to unavailable states of infinite energy. Thus, the reduction to an advection problem demonstrates immediately that there can be no stable steady configurations of the original vortices. This statement goes well beyond linear stability theory. We suggest that this mode of analysis can be applied also to the conventional vortex street problem and thus provide an alternative, geometrical route to the full nonlinear stability analysis of that configuration, which is known to be very demanding analytically (Kochin, Kibel & Roze 1964).

Phase-space plots and corresponding trajectories are similar for other cases that we have explored. By way of example, figure 11 shows the ζ-plane phase space for $(p, q) = (1, 5)$ and $X = L(3+10i)/40$. Regimes similar to those observed in figure 7 will be seen, although there are more of them. The general nature of trajectories, both in phase

FIGURE 10. Real-space trajectories of the three vortices corresponding to separatrices in the phase-space diagram of figure 7. Notation as in figure 9. The trajectories correspond and are labelled according to the separatrices indicated in figure 7. All motions are shown for the transition from saddle to saddle.

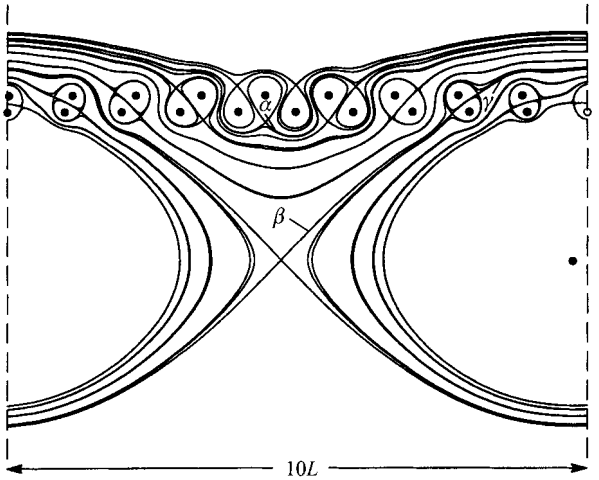

FIGURE 13. Phase space for $\Gamma_1:\Gamma_2:\Gamma_3 = 9:1:(-10)$, $\gamma = 2/5$, and $X = L(1+10i)/40$. The strip width is $10L$ and there are 20 advecting vortices (solid dots). Three separatrices are labelled (cf. figure 14).

space and in real space, is again similar to what we have seen in figures 7 and 9. The general nature of the separatrices is similar as well. Figure 12 shows two separatrices (labelled α and β in figure 11). The case $q = 5$ is interesting because it is the smallest denominator for which two values of the numerator, p, are allowed. Thus, in figure 13 we show the ζ-plane phase space for $(p, q) = (2, 5)$ and $X = L(1+10i)/40$. The main difference between figures 11 and 13 is that the lower row of advecting vortices contains just one vortex in the latter case but three in the former in accordance with the general theory given in §4. Figure 14 shows three real-space trajectories of the three vortices corresponding to the separatrices labelled α, β and γ in figure 13. Again the spatial complexity of the motions and the large number of periodic strips (10) over which these periodic motions extend have already emerged in our discussion of figures 9 and 12. The 'open dipoles' in the ζ-plane clearly have a major role to play in producing this dynamics.

Since we know the number of poles in a phase-space strip, it is possible to use simple ideas from the theory of analytic functions to count the number of saddle points (and hence states of steady translation) for a given rational γ, modulo 'accidental' degeneracies due to symmetries. For a general value of the linear impulse these vortex streets will translate with different velocities and will not be dynamically connected. There will be no separatrix joining them, i.e. the saddle points in the phase-space diagram will be homoclinic rather than heteroclinic. The two separatrices belonging to a given saddle will thus, generically, consist of a 'short branch' that loops a nearby vortex, and a 'long branch' that crosses the periodic boundary of the strip in the phase-space diagram. The short branch leads to relatively simple motions in which two vortices move as a pair. The long branch leads to the motions that extend over several strip widths as illustrated in figures 10, 12 and 14.

Based on explorations of various cases using the methods explained above we believe that the general, qualitative nature of the motion has been elucidated in all cases of rational γ. All motions (except for the separatrix motions) are periodic, and it always appears possible to find motions in which two of the base vortices will become separated by $2q$ (or q or $q/2$) periodic strip widths during one period.

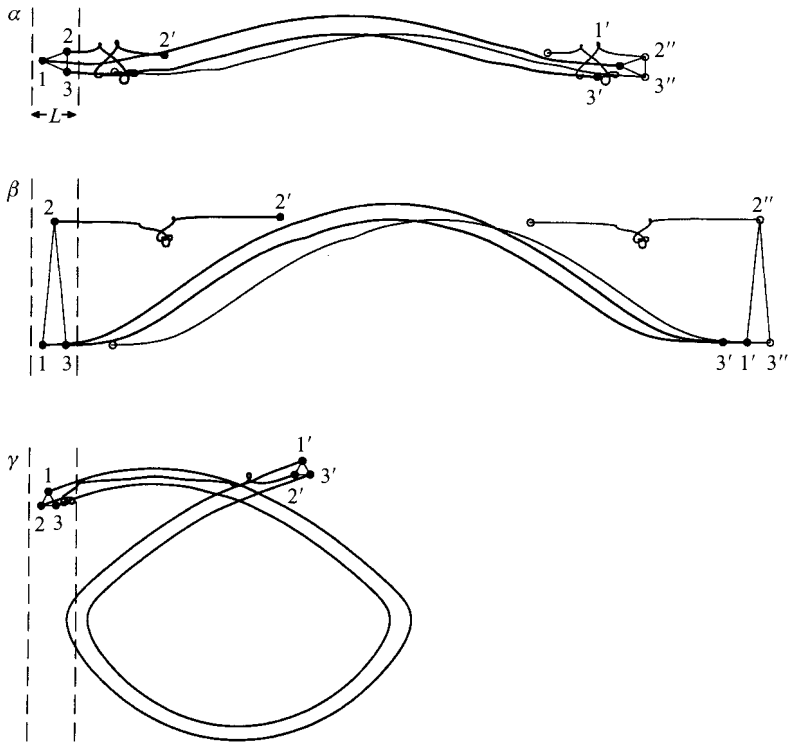

FIGURE 14. Real-space trajectories of the three vortices corresponding to the three separatrices α, β and γ in the phase-space diagram of figure 13. Notation as in figure 9. All motions are shown for the transition from saddle to saddle.

6. The case of irrational γ

In general γ will, of course, be irrational. The procedure given in §4 for rational γ does not immediately generalize and, in fact, seems to suffer a convergence problem if one considers a sequence of rational approximants, p_i/q_i, approaching the irrational γ ever more closely. For each of these the construction in §4 may be worked out. The problem is that the denominators in the series of rational approximants, i.e. the q_i, may fluctuate considerably, so that one is led to consider successive strips and vortex patterns that do not seem to be related or to be converging to a final result in any simple way.

The results obtained in §4 suggest that there is a mapping onto an advection problem for a passive particle in the field of a system of fixed vortices that belong to one of three infinite families. First, there should be a set of vortices of circulation $-\Gamma_3$ at regularly spaced locations $0, \pm L, \ldots$. Secondly there should be a set of vortices of circulation $\Gamma_3/(\gamma+\frac{1}{2}) = -\Gamma_3^2/\Gamma_1$ located at $(X+nL)/(\gamma+\frac{1}{2})$, $n = 0, \pm 1, \ldots$. Finally, there should be a family of vortices of circulation $-\Gamma_3/(\gamma-\frac{1}{2}) = -\Gamma_3^2/\Gamma_2$ at $(X+nL)/(\gamma-\frac{1}{2})$, $n = 0, \pm 1, \ldots$. Whereas for rational γ these three rows are a repeat of a basic pattern in a strip with a width that is a multiple of the given strip width, for irrational γ no such strip exists. The incommensurability of the spacings in the three rows means that an infinite system is required.

The same result is obtained analytically (and thus provides a different and maybe even simpler approach to the results in §4) if one works directly with the infinite series describing the mutual vortex interactions rather than summing them into cotangents as we did above. Within each series one has terms of the form $(z_1-(z_2+nL))^{-1}$ to

account for the influence of base vortex 2 and its periodic images on base vortex 1. There is an infinite sum on integers n for each such term. Within the sums, assuming convergence is assured, the scalings in (2.2) can now be shifted from denominator to numerator, and there can be absorbed in a rescaling of the vortex strength precisely as in the analysis of three-vortex motion on the unbounded plane (Aref 1989). The end result is exactly as stated in the preceding paragraph.

The phase-plane streamline pattern of the infinite system of fixed vortices is quite complex. We have already seen in the case of rational γ that the dipole-like structures around two close vortices of opposite sign usually are not closed. In the case of irrational γ it appears furthermore that, in general, *no two dipoles will be connected.* Hence, there will be an infinity of regimes, and since the return of a phase-space trajectory through a periodic boundary is precluded, only the ζ-motions confined to the vicinity of a single vortex will be bounded and periodic. Hence, most of the real-space motions will resemble the trajectories in figures 12 and 14, but will not be periodic (with or without the assistance of periodic images). Only motions for which the initial configuration has two of the vortices sufficiently close so that they 'move as a pair' will display periodicity.

7. Comparison with experiments by Williamson & Roshko

In order to compare the solutions obtained for a point vortex model with experimental results several problems must be addressed. Some of these have been known for many years since the well-known stability theory of conventional 'two-vortices-per-period' vortex streets was first proposed by von Kármán (see, for example, Lamb 1932, §156). First, in addition to the mutual interaction of the vortices as captured in the model treated here, a real wake has a mean flow that advects the vortices downstream. One might attempt to include that flow by adding the potential flow about a cylinder to the mutual interactions of the vortices, but in the present case the oscillation of the cylinder introduces additional complications. Even ignoring the oscillations, downstream variation of the mean flow implies that the periodic strip width used in the temporal model problem should be variable when the results are translated to the spatial problem. Second, the real wake is semi-infinite rather than doubly infinite as assumed in the point vortex model. Even ignoring the mean flow, or assuming it to be simply a constant advecting velocity, the periodicity assumption can only begin to be valid as one travels some distance downstream along the wake. Unfortunately, viscous effects (also ignored) have then had time to act, and the location, concentration and two-dimensionality of the vortices in the wake can be called into question. Finally, the precise values of the circulations is typically not known in the experiment, although it is reasonable to assume that the total circulation of all vortices shed during a full cycle is zero. It follows from all these caveats that any comparison of our model results with experiments will be quite qualitative, and while the model results clearly can stand on their own merits, we feel that the modelling attempt to be undertaken in this section does increase the understanding of the experimental observations and suggests new experiments on the wake of an oscillating cylinder.

We decided to attempt a comparison of our model problem solutions with the experimental photographs of Williamson & Roshko (1988). Professors Roshko and Williamson have both kindly sent us original photos so that we might have as clear a record as possible for this task. Figure 15 summarizes our attempts at fitting one of our solutions to the experimental photograph appearing as figure 17(*c*) in Williamson &

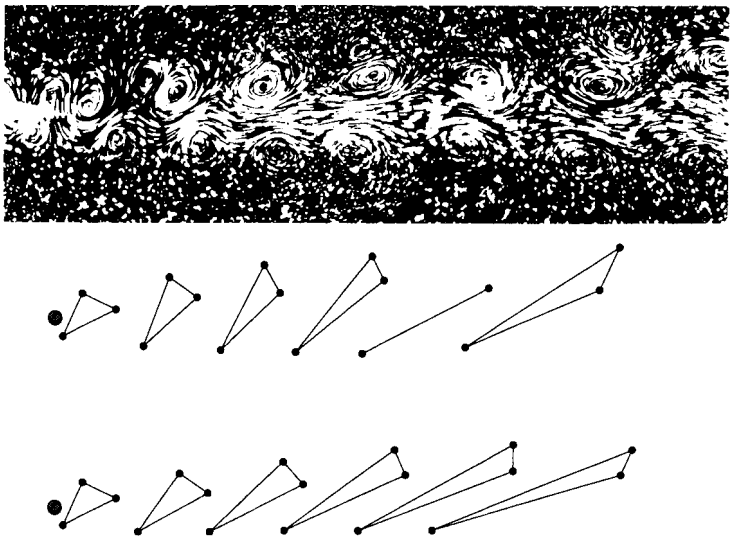

FIGURE 15. Comparison of flow visualization of the wake of an oscillating cylinder (Roshko & Williamson 1988) and point vortex model solutions. (*a*) Reproduction of a flow visualization. (*b*) Locations of vortex cores as determined from the photograph; note that for the fifth triple downstream we could not identify one of the vortices. (*c*) A 'best fit' analytical solution using the theory presented.

Roshko (1988). Panel (*a*) of figure 15 simply reproduces the experimental photograph. In panel (*b*) we have plotted the positions of the vortices as measured from the photograph. The triangles connect those vortices that appear to belong to the same shedding cycle. Panel (*c*) represents our attempt to reproduce the vortex motions of the experiment using the point vortex model. Here the triangles connect a set of 'base vortices', in the sense of the preceding discussion, at different instants of time.

In the previous sections, the model problem dealt only with the motion of point vortices in otherwise quiescent fluid. However, the experimental photo in figure 15(*a*) was produced by towing a transversely oscillating cylinder through water, with three vortices being shed for each cycle. We neglect any effect of the cylinder on the potential flow downstream, but to compare with experiment we need our coordinate system to translate with the cylinder. That is, the velocity of a vortex must now be due to its interaction with the other vortices plus an advection by a free-stream velocity equal and opposite to the cylinder translation velocity. Now, in order to produce the appropriate picture, we need to specify the translation velocity of the cylinder, the width of the periodic strip to be used for generating our model solution, the vortex strengths, and the initial vortex locations. We now mention how we chose these various parameters. The translation velocity and strip width can be determined from the relevant dimensionless parameters Re and L/D, where the Reynolds number Re is based on the cylinder's translation velocity U and diameter D, and L is the wavelength of the resulting cylinder motion. Williamson and Roshko (private communication) report $D = 1$ in., $Re = 275$, and $L/D = 6.0$. The periodic strip width is taken as the horizontal distance that the cylinder travels in one cycle, i.e. $6D$. We approximate the vortex strengths by using the empirical relationship $K/U^2 = A$ (see Birkhoff & Zarantonello 1957), where U is the free-stream velocity and K is the product of the shedding frequency and the circulation shed from one side of the cylinder. We take $A = 0.32$ (Koopman 1967), which was given for a stationary cylinder, but we use it here,

nevertheless, as an approximation. Owing to viscous effects one expects that about two-thirds of the circulation shed from one side of the cylinder ends up as the circulation associated with a shed vortex. The bottom-most vortex in each triangle (the only vortex shed from the bottom of the cylinder in one cycle) is thus assigned a positive circulation based on this empirical result. The value of the other two vortex strengths is now determined by γ, which is the only free parameter that we can use in an attempt to match our results to experiment. For figure 15(*c*) we have used $\gamma = \frac{1}{4}$, with the bottom vortex considered as vortex 2, i.e. the vortex strengths are taken to be in proportion $\Gamma_1 : \Gamma_2 : \Gamma_3 = 3 : 1 : (-4)$. Finally, the initial vortex positions are taken as those in the first triangle on the left in figure 15(*b*). We now integrate numerically in time through one full cycle of the cylinder oscillation, record the vortex locations, integrate through another cycle, again record the vortex locations, and so on to create the picture in figure 15(*c*). Note that we are using the doubly periodic solutions discussed previously – no attempt has been made to include image vortices in the cylinder, or to account for a wake flow of any kind.

It is difficult to claim too much for the comparison presented in figure 15. However, we do believe that the following conclusions are merited: (i) The relative motion of three vortices shed during a cycle in the wake of an oscillating cylinder resemble the 'unbounded' motions for the point vortex model problem in the sense that the base vortices separate ever further as the motion evolves, i.e. downstream distance between vortices shed in the same cycle grows in time; the model problem explains the existence and likelihood of this type of motion. (ii) The full solution of the model problem suggests that there are several other regimes of motion, counterparts of which have not so far been seen in the experiments; the model shows where in the (γ, X) parameter space one might expect to find these motions, but it cannot, of course, say anything about how to oscillate the cylinder in order to produce appropriate initial conditions for the vortices. (iii) The full set of solutions to the point vortex problem clearly shows that the amount of mixing along the wake can be varied considerably depending on how the vortices are positioned immediately after one shedding cycle; this observation suggests that considerable control can be exercised over mixing in the wake of an oscillating cylinder by judicious choice of shedding frequency, amplitude and oscillation direction.

It would clearly be a very interesting and worthwhile step to establish additional correspondence between experimental parameters that govern three-vortex-per-cycle shedding patterns and the regimes of motion brought to light by the present analysis. Very sensitive dependence of wake evolution on shedding conditions may be observable close to conditions for which the ratio of two vortex strengths is an irrational number that is hard to approximate by rationals, such as the golden mean. However, the motion is always integrable regardless of the value of γ.

A preliminary report on this work was presented at the annual meeting of the APS Division of Fluid Dynamics in Atlanta, GA, November 1994 (Stremler & Aref 1994). The support of NSF grant CTS-9311545 is gratefully acknowledged. M.S. also acknowledges the support of an ONR Fellowship.

REFERENCES

AREF, H. 1979 Motion of three vortices. *Phys. Fluids* **22**, 393–400.

AREF, H. 1983 Integrable, chaotic, and turbulent vortex motion in two-dimensional flows. *Ann. Rev. Fluid Mech.* **15**, 345–389.

AREF, H. 1985 Chaos in the dynamics of a few vortices – fundamentals and applications. In *Theoretical and Applied Mechanics* (ed. F. I. Niordson & N. Olhoff), pp. 43–68. North-Holland.

AREF, H. 1989 Three-vortex motion with zero total circulation: Addendum. *Z. Angew. Math. Phys.* **40**, 495–500.

AREF, H. 1995 On the equilibrium and stability of a row of point vortices. *J. Fluid Mech.* **290**, 167–181.

AREF, H., ROTT, N. & THOMANN, H. 1992 Gröbli's solution of the three-vortex problem. *Ann. Rev. Fluid Mech.* **24**, 1–20.

BIRKHOFF, G. & FISHER, J. 1959 Do vortex sheets roll up? *Rend. Circ. Mat. Palermo* **8**, 77–90.

BIRKHOFF, G. & ZARANTONELLO, E. 1957 *Jets, Wakes and Cavities*. Academic.

BLOMBERG, D. C. 1984 Point vortex models of a forced shear layer. MSc thesis, Brown University.

COUDER, Y. & BASDEVANT, C. 1986 Experimental and numerical study of vortex couples in two-dimensional flows. *J. Fluid Mech.* **173**, 225–251.

ECKHARDT, B. 1989 Integrable four-vortex motion. *Phys. Fluids* **31**, 2796–2801.

ECKHARDT, B. & AREF, H. 1988 Integrable and chaotic motions of four vortices II: Collision dynamics of vortex pairs. *Phil. Trans. R. Soc. Lond.* A **326**, 655–696.

GRIFFIN, O. M. & RAMBERG, S. E. 1974 The vortex-street wakes of vibrating cylinders. *J. Fluid Mech.* **66**, 553–576.

GRIFFIN, O. M. & RAMBERG, S. E. 1976 Vortex shedding from a cylinder vibrating in line with an incident uniform flow. *J. Fluid Mech.* **75**, 257–271.

GRIFFIN, O. M., SKOP, R. A. & KOOPMAN, G. H. 1973 The vortex-excited resonant vibrations of circular cylinders. *J. Sound Vib.* **31**, 235–249.

GRÖBLI, W. 1877 *Specielle Probleme über die Bewegung geradliniger paralleler Wirbelfäden*. Zürich: Zürcher und Furrer.

HONJI, H. & TANEDA, S. 1968 Vortex wakes of oscillating circular cylinders. *Rep. Res. Inst. Appl. Mech.* **16**, 211–222.

KOCHIN, N. E., KIBEL, I. A & ROZE, N. V. 1964 *Theoretical Hydrodynamics*. Interscience.

KOOPMAN, G. H. 1967 The vortex wakes of vibrating cylinders at low Reynolds numbers. *J. Fluid Mech.* **28**, 501–512.

LAMB, H. 1932 *Hydrodynamics*, 6th edn. Dover.

NOVIKOV, E. A. 1975 Dynamics and statistics of a system of vortices. *Sov. Phys. JETP* **41**, 937–943.

ONGOREN, A. & ROCKWELL, D. 1988 Flow structure from an oscillating cylinder II: Mode competition in the near wake. *J. Fluid Mech.* **191**, 225–245.

ROTT, N. 1989 Three-vortex motion with zero total circulation. *Z. Angew. Math. Phys.* **40**, 473–494.

ROTT, N. 1990 Constrained three- and four-vortex problems. *Phys. Fluids* A **2**, 1477–1480.

ROTT, N. 1994 Four vortices on doubly periodic paths. *Phys. Fluids* **6**, 760–764.

STREMLER, M. A. & AREF, H. 1994 Motion of three vortices in a periodic strip. *Bull. Am. Phys. Soc.* **39**, 1890.

SYNGE, J. L. 1949 On the motion of three vortices. *Can. J. Maths* **1**, 257–270.

WILLIAMSON, C. H. K. & ROSHKO, A. 1988 Vortex formation in the wake of an oscillating cylinder. *J. Fluids Struct.* **2**, 355–381.